ARTICLE

Buckysomes: Fullerene-Based Nanocarriers for Hydrophobic Molecule Delivery

Ranga Partha, Linsey R. Mitchell, Jennifer L. Lyon, Pratixa P. Joshi, and Jodie L. Conyers*

Department of Internal Medicine, The University of Texas Health Science Center at Houston, 6431 Fannin Street, Houston, Texas 77030

ABSTRACT We report the preparation and preliminary *in vitro* studies of nanocarriers termed "buckysomes," which are self-assembled, spherical nanostructures composed of the amphiphilic fullerene AF-1. By inducing AF-1 self-assembly at an elevated temperature of 70 °C, dense spherical buckysomes with diameters of 100—200 nm were formed, as observed by electron microscopy and dynamic light scattering. The amphiphilic nature of AF-1 results in the formation of many hydrophobic regions within the buckysomes, making them ideal for embedding hydrophobic molecules to be tested in a drug delivery scheme. After confirming the cellular internalization of buckysomes embedded with the hydrophobic fluorescent dye 1,1′-dioctadecyl-3,3,3′,3′-tetramethylindocarbocyanine perchlorate, we embedded paclitaxel, a highly hydrophobic anticancer drug. The *in vitro* therapeutic efficacy of the paclitaxel-embedded buckysomes toward suppression of MCF-7 breast cancer cell growth was compared to that of Abraxane, a commercially available, nanoparticle-albumin-bound formulation of paclitaxel. Notably, the paclitaxel-embedded buckysomes demonstrated a similar efficacy to that observed with Abraxane in cell viability studies; these results were confirmed microscopically. Moreover, negative control studies of MCF-7 viability using empty buckysomes demonstrated that the buckysomes were not cytotoxic. The results of our studies suggest that buckysomes prepared from self-assembly of AF-1 at 70 °C are promising nanomaterials for the delivery of hydrophobic molecules.

KEYWORDS: paclitaxel · AF-1 · buckysome · self-assembly · amphiphilic fullerene · drug delivery

Nanocarriers are nanoscale materials that can carry therapeutic payloads to biogenic sites. Such materials include nanoparticles, lipoproteins, micelles, dendrimers, nanoshells, functionalized nanotubes, and polymeric microspheres, all of which are of great interest for applications in therapeutic drug delivery.[1] Of these nanocarrier materials, phospholipid-based liposomes have been studied the most extensively;[2] liposomes have been successfully utilized not only in drug delivery but also in a variety of other biomedical applications including diagnostic imaging,[3,4] gene therapy,[5] and biosensing.[6] Nevertheless, the structure of conventional phospholipid liposomes substantially limits their applications. In particular, the self-assembly of phospholipids in aqueous solution creates a hydrophilic interior compartment in the resulting liposomes. Though these compartments can encapsulate ~mM concentrations of hydrophilic drugs,[7] they are insufficient for the encapsulation of hydrophobic molecules. Several hydrophobic-interior nanocarriers have been reported,[8−12] but none of these nanocarriers have progressed to clinical testing, and they suffer from low payload capacities and restricted bioavailability of their encapsulated hydrophobic molecules.[13,22] Therefore, fundamental studies aimed at synthesizing and understanding a nanocarrier system that is capable of carrying large amounts of hydrophobic molecules should be undertaken.

One promising alternative to phospholipid liposome nanocarriers is a nanocarrier composed of carbon nanostructures. Two allotropes of carbon, the nanotube and the fullerene, have recently received much attention as potential components in biological applications. Some discrepancy exists in the literature regarding the potential toxicity of fullerenes *in vivo*. For example, studies by Oberdörster *et al*. indicated that water-solubilized C_{60} fullerenes can be somewhat cytotoxic in living organisms;[14,15] however, the tetrahydrofuran solvent used during the solubilization procedure might have contributed to the observed toxicity. In contrast, Gharbi *et al*. have reported that underivatized C_{60} fullerenes exhibit no cytotoxicity in rodents.[16] Moreover, the aqueous solubility and biocompatibility of fullerenes may be further increased by covalently modifying their surfaces with various hydrophilic functional groups. Such modified fullerenes have been used to create vesicular[17] and spherical structures.[18−20] Notably, Hirsch *et al*. have synthesized a set of water-soluble, amphiphilic fullerene compounds[21−25] that self-assemble in aqueous solution to form

*Address correspondence to Jodie.L.Conyers@uth.tmc.edu.

Received for review May 30, 2008 and accepted August 12, 2008.

Published online August 22, 2008.
10.1021/nn800422k CCC: $40.75

Figure 1. (A) Cryo-EM image showing the solid, dense spherical structures obtained upon self-assembly of AF-1 monomers at an elevated temperature of 70 °C; scale bar = 100 nm. (B) Freeze-fracture micrograph (scale bar = 200 nm) and (C) transmission electron micrograph (scale bar: = 500 nm) confirm the spherical morphology of the buckysomes in panel A and also indicate a similar size profile. All three images were obtained from the same buckysome sample.

spherical vesicles referred to as "buckysomes," which are similar to conventional phospholipid liposomes both in size and in their vesicular morphology.[23] One such amphiphilic fullerene capable of forming buckysomes is the molecule AF-1, which consists of a C_{60} fullerene modified with a Newkome-like dendrimer unit containing 18 carboxylic acid groups. Five other positions on the fullerene are occupied by dodecyl malonates, which are positioned octrahedrally to the dendritic group (see Figure 1 in ref 26).

In a recent collaborative effort with Dr. Hirsch and colleagues, we have extensively characterized vesicular spherical buckysomes formed by self-assembly of AF-1.[26] We observed both unilamellar and multilamellar vesicles with diameters of 50−150 and >400 nm, respectively, similar in size to some phospholipid liposomes. The bilayer thickness of the vesicular buckysomes is ~6.5 nm, as evidenced by transmission electron microscopy (TEM) and cryogenic electron microscopy (cryo-EM) images. Importantly, we observed that by varying the experimental conditions for AF-1 self-assembly (*e.g.*, pH, buffer composition) additional morphologies are attained, including nanoscale rods, micellar structures, and complex networks of tubes.[26] These findings motivated us to optimize the self-assembly conditions for AF-1 with the goal of creating buckysome nanocarriers for hydrophobic molecule delivery, and herein we report the preparation of dense, spherical buckysomes possessing internal hydrophobic pockets that effectively encapsulate hydrophobic molecules. These structures were created by inducing AF-1 self-assembly at a temperature of 70 °C, and their morphology differed markedly from the vesicular structures previously observed for buckysomes formed from AF-1 self-assembly at room temperature. (Although these new structures do not possess the vesicular morphology characteristic of traditional buckysomes, we will refer to them as "buckysomes" throughout this report.) The morphology of the buckysomes was characterized by means of TEM, cryo-EM, and freeze-fracture microscopy, as well as dynamic light scattering. To demonstrate the buckysomes' uptake and release of hydrophobic materials, we encapsulated the hydrophobic fluorescent probe 1,1′-dioctadecyl-3,3,3′,3′-tetramethylindocarbocyanine perchlorate (DiI) in the buckysomes. The internalization of DiI-loaded buckysomes in cells was monitored with fluorescence microscopy.

We then loaded the buckysomes with paclitaxel, a hydrophobic anticancer drug approved by the U.S. Food and Drug Administration (FDA) for the treatment of a variety of tumors resulting from breast, ovarian, and head/neck cancers.[27,28] Previous studies have explored the encapsulation of paclitaxel in liposome-based formulations[29,30] to alleviate patient discomfort associated with traditional nonaqueous methods of paclitaxel administration,[31,32] but the liposomes' uptake by phagocytes and poor physical stability have considerably hindered the development of such lipid-based nanocarriers.[33] To evaluate the buckysomes as a possible alternative nanocarrier for paclitaxel, we assessed the therapeutic efficacy of paclitaxel-embedded buckysomes (PEBs) toward MCF-7 breast cancer cell growth both through cell viability assays and optical microscopy. These results were compared to those obtained using Abraxane, a nanoparticle-albumin-bound form of paclitaxel manufactured by AstraZeneca and currently used for cancer treatment. We found that PEBs were nearly as effective as Abraxane for preventing MCF-7 cell growth at the paclitaxel concentrations tested. Differences in cell internalization between PEBs and Abraxane are also discussed. Our findings demonstrate that buckysomes prepared under the experimental conditions described herein show much promise for use as nanocarriers for the delivery of paclitaxel and other hydrophobic molecules.

RESULTS AND DISCUSSION

Preparation and Electron Microscopy Characterization of Buckysomes. In a previous study,[26] we described the effects of pH and various aqueous buffers (solvent) on the self-assembly of AF-1 into buckysomes. Cyro-EM images of these previously prepared buckysomes reveal

the formation of vesicular nanostructures by instantaneous self-assembly. Both unilamellar and multilamellar vesicular structures were formed from AF-1 self-assembly at room temperature in 10 mM citrate buffer at pH 7.4.

In the present study, we explored the effects of varying the temperature used during AF-1 self-assembly. Buckysomes were prepared at an elevated temperature of 70 °C in the present study, in contrast with the room-temperature conditions used in the previous study. All other variables in the self-assembly process including pH, buffer composition, and method of preparation remained unchanged. We note that for both the room-temperature and elevated-temperature preparations, the self-assembly of AF-1 into buckysomes was rapid and spontaneous, requiring only the hydration of dry AF-1 with citrate buffer and brief vortex cycles over a span of 10 min (see Materials and Methods). The resulting buckysomes required no extrusion or other isolation procedures typically used during preparation of conventional phospholipid liposomes. Importantly, the self-assembly of AF-1 occurred readily in aqueous solution at physiological pH and did not require the use of any organic solvents, as opposed to conventional liposome preparations, which typically require dissolution of precursor lipids in chloroform or other organics to create a lipid film, followed by removal of the organic solvent prior to hydration of the film in aqueous solvent. In agreement with our observations of AF-1 self-assembly in aqueous solution, Hirsch *et al*. have previously noted that the dendritic headgroups of amphiphilic fullerenes have a much greater hydration capacity than do phospholipids.[22]

The samples prepared at elevated temperature were analyzed by three different complementary microscopic techniques: cryo-EM, freeze-fracture microscopy, and TEM. A representative cryo-EM image is shown in Figure 1A. This type of electron microscopy was used because it preserves the native three-dimensional structure of samples.[34] Notably, the image in Figure 1A shows spherical structures that differ substantially from the vesicular structures previously observed for room-temperature self-assembly. These new structures were 100−200 nm in diameter with a dense interior. Freeze-fracture microscopy images (Figure 1B) complement the cryo-EM data by showing spherical structures of similar size. (The few rodlike structures apparent in the image are fused buckysomes, which are sometimes formed during freeze-fracture microscopy sample preparation.) In addition, the negative-stain TEM image in Figure 1C reveals structures of the same size as those observed in Figures 1A and B.

Importantly, the dark contrast observed in the interior of the structures in Figure 1A likely corresponds to the presence of densely assembled aggregates of AF-1 monomers,[35,36] indicating that the self-assembly process at 70 °C did not produce the bilayered vesicular buckysome structures observed in room-temperature self-assembly. We have performed tilt measurements at +45° and −45° using cryo-EM and found this dark contrast to be uniform inside the spherical buckysomes (data not shown). This observation again indicates that the interior is composed of a dense network of AF-1 aggregrates. Since all other experimental parameters were maintained constant between the two preparations, the elevated temperature must have induced the changes in buckysome morphology observed here. The exact mechanism by which the elevated self-assembly temperature promoted the formation of these dense buckysomes remains unclear at present. Though the temperature-dependent self-assembly of modified fullerenes has not been extensively explored in the literature, the effects of temperature on lipid polymorphism, in particular changes induced in liposome structures as a result of increasing temperature, have been reported.[37,38] Additionally, the increase in entropy induced by increasing the self-assembly temperature might also contribute to the buckysomes' formation, as such thermodynamic changes are known to influence lipid bilayer and vesicle formation.[39]

The orientation of AF-1 monomers within these dense buckysomes is also unknown, and could be one of many possible morphologies, as amphiphilic fullerenes have been shown to self-assemble into many different types of structures. For example, a previous report by Hirsch *et al*.[25]demonstrated that an amphiphilic fullerene derived from AF-1 can form double-layered aggregates as well as globular micelles. Because we have previously demonstrated that AF-1 can form a variety of micellar structures,[26] we propose here that the filled interior contains a complex arrangement of several micellar subunits, though it is unclear at this point whether these micellar subunits are spherical or sheet-like. Hydrophobic pockets within these micellar subunits most likely provide a favorable environment for small hydrophobic molecules to reside in (*vide infra*).

Alternatively, the buckysomes' interior could possibly contain compressed mutliple bilayers, similar to those observed in spherulite structures.[40] However, our freeze-fracture images do not support this theory, because these images do not feature concentric patterns of bilayers. To elucidate the three-dimensional interior structure of the dense buckysomes, we plan to further characterize them by means of cryo-electron tomography[41−43] as well as small-angle neutron scattering combined with small-angle X-ray scattering.[44] By labeling buckysomes with hydrophobic gold particles to perform energy dispersive X-ray spectroscopy mapping,[45] additional structural details can also be revealed. Regardless of the actual orientation of AF-1 monomers, the interior of the buckysome structures prepared at elevated temperature should contain many hydrophobic regions due to the presence of the

densely aggregated, amphiphilic fullerenes. We hypothesized that these hydrophobic regions might serve as pockets for the encapsulation of hydrophobic molecules, and to test this hypothesis we embedded both a hydrophobic dye and the hydrophobic drug paclitaxel within the buckysomes (*vide infra*).

Cellular Internalization of Buckysomes Embedded with a Hydrophobic Fluorescent Dye. One promising application of our dense buckysomes is their use as nanocarriers to deliver hydrophobic drugs. An example of such a hydrophobic drug is paclitaxel, a taxane that is an effective choice for chemotherapy in treating breast, ovarian, and other types of cancer.[27,28] Paclitaxel promotes the polymerization of tubulin and therefore disrupts normal microtubule dynamics. This disruption affects the cell division process in tumor cells, inducing programmed cell death.[46] However, paclitaxel is an extremely hydrophobic drug and poses severe delivery problems in biological systems. Previously, paclitaxel delivery has been achieved using polyethoxylated castor oil (Cremophor EL), but due to unwanted side-effects caused by the castor oil solvent,[31,32] water-soluble paclitaxel carriers are more desirable. To this end, lipid-based formulations of paclitaxel have been investigated,[29,30] but the development of such formulations has been limited by their poor physical stability and uptake by phagocytes, as noted above. A more effective alternative to lipid-based paclitaxel formulations is the FDA-approved, water-soluble compound Abraxane, which contains paclitaxel bound to human serum albumin in a nanoparticle colloid.[47] Clinical trials have clearly established that Abraxane has several therapeutic advantages over Cremophor EL, including a lack of side effects, rapid infusion rate, and high paclitaxel maximum tolerated dose.[48]

Like Abraxane, our buckysomes are water-soluble, and their hydrophobic character permits their exploration as potential nanocarriers for the delivery of paclitaxel and other hydrophobic molecules. For this reason, we sought to evaluate the ability of the buckysomes prepared at elevated temperature to uptake hydrophobic molecules, with the ultimate goal of assessing the buckysomes' potential as a nanocarrier for hydrophobic drugs. To determine whether hydrophobic drugs such as paclitaxel could be embedded into our buckysomes and subsequently internalized into cells, we first embedded the hydrophobic fluorophore DiI into the buckysomes and monitored its internalization *in vitro*. Mouse macrophages were incubated with DiI-embedded buckysomes and later fixed and stained. Figure 2 shows brightfield (panels 1 and 2) and corresponding fluorescence (panels 3 and 4) images of the macrophages. Panel 1 shows the morphology of the fixed macrophages without fluorescence. Panel 2 is a superimposed brightfield image showing 4′,6-diamidino-2-phenylindole (DAPI) and DiI staining. The internalization of DiI-embedded buckysomes is clearly

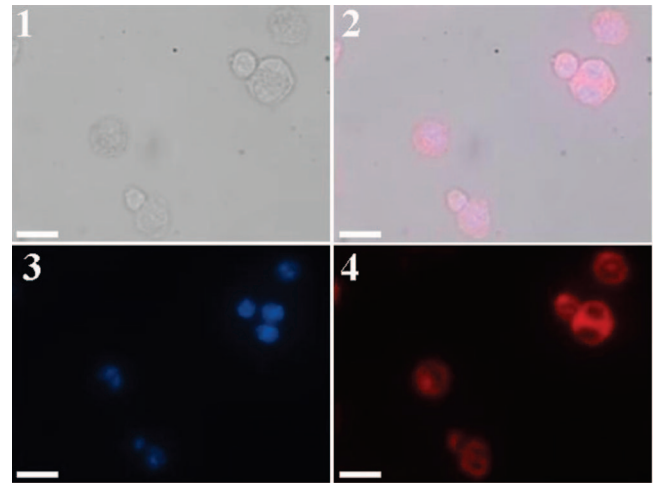

Figure 2. Fluorescence micrographs of fixed and stained mouse macrophages, which were exposed with DiI-embedded buckysomes. The cells were washed several times with PBS before counterstaining nuclei with DAPI: (1) phase contrast image; (2) brightfield image showing superimposed DAPI and DiI emission; (3) DAPI emission at 460 nm, showing the location of macrophage nuclei; (4) DiI emission at 570 nm, showing the presence of DiI-embedded buckysomes inside the cytoplasm. The scalebar is 20 μm in all four images.

confirmed in panel 2. Panel 3 shows DAPI fluorescence the macrophage nuclei, and panel 4 shows that DiI was internalized in the cytoplasm of the macrophages, as indicated by the close proximity of intense DiI fluorescence (red) to the location of the nuclei (blue) in panel 3. These results served as proof-of-concept that buckysomes embedded with hydrophobic molecules could be internalized by cells. Conventional liposomes of similar size and overall structure to our buckysomes are known to be internalized by cells through endocytosis that is not receptor-mediated,[49−52] and we believe that our buckysomes were internalized by the macrophages through a similar entry mechanism.

To further confirm that the buckysomes were internalized by cells and not merely cell-associated, we incubated 6-aminofluorescein-labeled buckysomes with A431 epidermoid carcinoma cells. The cells were then fixed and counterstained with wheat gluten AlexaFluor 594, which binds specifically to lipophilic regions (*i.e.*, cell membranes), and Hoescht 33342 nuclei stain. The resulting fluorescence image (Figure 3A) clearly shows internalization of the fluorescein-labeled buckysomes (green) inside the cells (cell membranes are red and nuclei are blue). The intense pink spot at the lower right of the image is an artifact most likely caused by a lipid-rich region in the cell membrane. Notably, no change in localization of the buckysomes was observed following several washes with phosphate-buffered saline. These results, in combination with the DiI-embedded buckysome data described in Figure 2, suggested that paclitaxel might be successfully embedded in the buckysomes, and that the resulting PEBs might be internalized by cancerous cells.

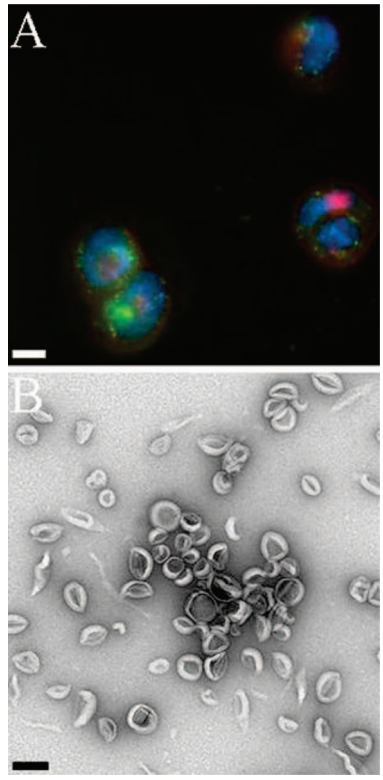

Figure 3. (A) Fluorescence microscopy of A431 human epidermoid carcinoma cells incubated with 6-aminofluorescein-labeled buckysomes (green) for 18 h, showing cell internalization. Cells were fixed and counterstained with Hoescht 33342 (nuclei; blue) and AlexaFluor 594 (membranes; red). The image shown here is that of fluorescein (518 nm), Hoescht (461 nm), and Alexa-Fluor (618 nm) emissions superimposed. The scale bar is 10 μm. (B) TEM image of paclitaxel-embedded buckysomes (PEBs). The PEBs were visualized with 1% uranyl acetate staining. The scale bar is 200 nm.

Notably, the observation that buckysomes were internalized by both cells and macrophages *in vitro* might suggest that the nanocarriers would be internalized by macrophages *in vivo*, thus reducing the amount of therapeutics available for treatment of cancerous cells. However, we note that the *in vitro* macrophage studies conducted here differ markedly from conditions that would be encountered *in vivo*. More specifically, the macrophages used here were subjected to incubation with a high concentration of buckysomes for 18 h, without fluid motion or other disturbance (see Methods and Materials). In contrast, both the macrophages and drug-loaded buckysomes would be in constant, rapid motion in blood serum under *in vivo* conditions. We believe that this markedly reduced "contact time" between the two species would substantially hinder the uptake of buckysomes by macrophages *in vivo*, and we are currently outlining *in vivo* studies in murine models to confirm this hypothesis. Furthermore, the size of liposomes is well-known to influence their *in vivo* circulation time, and in particular liposomes larger than 200 nm are considered to be cleared faster by the reticuloendothelial system than are smaller liposomes.[53] Because our PEBs have an average size of around 128 nm (see Supporting Information, Figure 1), we can expect them to avoid macrophage uptake to some degree *in vivo*. The size range of our PEBs is also appropriate for exploiting the enhanced permeability and retention effect in solid tumors.[54]

Following the successful cell internalization of the DiI-embedded buckysomes, we proceeded to embed paclitaxel into the buckysomes. High performance liquid chromatography (HPLC) data (see Supporting Information) showed that the molar ratio of AF-1/paclitaxel was 1:3 with a maximum percentage encapsulation of 53%. Figure 3B is a TEM image of PEBs, demonstrating that the morphology of the PEB structures remained the same as that of the empty buckysomes shown in Figure 1C. This microscopic evidence was confirmed with dynamic light scattering experiments, which indicated an average PEB diameter of 128 ± 5 nm (see Supporting Information). Since the morphology of the PEBs did not appear to differ substantially from that of the empty buckysomes (i.e., those without paclitaxel embedded), we expected that the PEBs would be internalized by cells in a manner similar to that observed for the fluorescein-labeled, empty buckysomes.

***In Vitro* Cell Viability of MCF-7 Cells Treated with PEBs.** To determine the efficacy of PEBs as an anticancer nanocarrier, we performed *in vitro* cell viability assays with MCF-7 breast cancer cells using the trypan blue dye exclusion method. Upon cell death, the cell membrane becomes permeable, thereby allowing the trypan blue dye to enter and stain the nonviable cells, which are analyzed with a cell viability analyzer. Abraxane was used as a positive control, and empty buckysomes as well as citrate buffer containing no buckysomes were used as negative controls. MCF-7 cells were incubated with the samples for different time intervals ranging from 24−96 h at 37 °C. We did not see any pronounced cell suppression at 24 h (data not shown), and normal cell death was prevalent at 96 h (data not shown). However, the effect of paclitaxel on cell growth was clearly seen at 48 and 72 h (Figure 4). In the negative control studies (Figure 5, columns A and B), the concentrations of citrate buffer and AF-1 were 0.48 mM and 59.53 μg/ml, respectively. The number of viable cancer cells increased between 48 and 72 h in both negative control studies, consistent with normal cell growth during this time period. Importantly, the empty buckysomes (B) did not hinder cell growth as compared to the buffer (A), demonstrating that the bucksyomes themselves were not cytotoxic. These results are in agreement with our previous studies, in which we established that vesicular buckysomes are not cytotoxic.[26]

For cell viability studies with PEBs and Abraxane positive controls, the final concentrations of paclitaxel incubated with the cells were 28.6 (Figure 4, columns C and D), 143 (columns E and F), and 714 ng/ml (columns G and H). Compared to the viability results obtained in the negative control studies, MCF-7 cell

growth was suppressed when paclitaxel was delivered using either PEBs (C, E, and G) or Abraxane (D, F, and H). The decrease in cell viability was more prominent at 72 h and with the highest concentration (714 ng/ml) of paclitaxel in both PEBs and Abraxane formulations. Interestingly, the results obtained with PEBs and Abraxane were quite comparable. However, the mode of cell internalization might differ between these two nanocarriers. Unlike the buckysomes, which are likely internalized by means of non-receptor-mediated endocytosis as described above, Abraxane transports paclitaxel across endothelial cells and to tumor sites by glycoprotein-mediated endothelial cell transcytosis of the paclitaxel-bound albumin.[55−58]

During the course of the MCF-7 cell viability assay (Figure 4) we simultaneously monitored the cells' morphological changes using optical microscopy. The images (Figure 5) clearly correlated with the results obtained in the viability studies. MCF-7 cells grow in aggregates *in vitro*,[59] and no marked difference was observed in the cell density between the buffer (Figure 5, panel 1) and empty buckysome (panel 2) negative controls. These observations again confirmed that the empty buckysomes were not cytotoxic. The images in panels 1 and 2 differ remarkably from those observed upon delivery of 714 ng/ml of paclitaxel by both the PEBs (panel 3) and Abraxane (panel 4) at 72 h. In both of these panels, MCF-7 cells are more sparse in appearance, indicating that the delivered paclitaxel hindered the cell division process. We observed similar results at 48 h (data not shown).

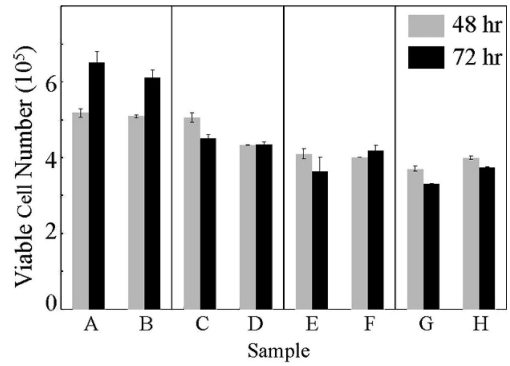

Figure 4. Trypan blue dye-based cell viability assay of MCF-7 cells. Samples were incubated for a period of 48 (gray bars) and 72 h (black bars) at 37 °C. Negative controls were 0.48 mM citrate buffer (A) and empty buckysomes (B). The concentration of paclitaxel in the PEBs was 28.6 (C), 143 (E), and 714 ng/ml (G). The comparative positive control was Abraxane, with identical paclitaxel concentrations in columns D, F, and H, respectively.

CONCLUSION

In summary, we have developed a new fullerene-based nanocarrier capable of delivering hydrophobic molecules. Using AF-1, a water-soluble modified fullerene that has previously been shown to self-assemble intro vesicular buckysomes, we prepared new buckysome structures through self-assembly at 70 °C in an aqueous environment. These new buckysome structures were spherical with diameters of 100−200 nm and contained hydrophobic interiors composed of densely aggregated AF-1 monomers. The buckysomes' physical and structural properties were ideal for the encapsulation of hydrophobic molecules. Paclitaxel, an extremely hydrophobic anticancer drug, was chosen as a model delivery molecule after we visualized the internalization of buckysomes inside cells using fluorescence tracking of an embedded hydrophobic molecular dye. We successfully loaded paclitaxel into the buckysomes and monitored their structure and stability with different types of electron microscopy. Preliminary *in vitro* cell viability assays indicated that the paclitaxel-embedded buckysomes were comparable with Abraxane for suppressing MCF-7 breast cancer cell growth. The viability data was well supported by continuous microscopic observation of live cell growth. In attempts to further optimize the hydrophobicity and encapsulation efficiency of the buckysomes' interiors, we plan to explore the modification of AF-1 with lipid chains of varying length. Future studies are also aimed at functionalizing the buckysomes' surfaces with targeting molecules to promote site-specific delivery. Our current work suggests that PEBs might be an exciting prospect for nanocarrier-based *in vivo* cancer therapy, and we are currently investigating the therapeutic efficacy of PEBs in a mouse tumor model.

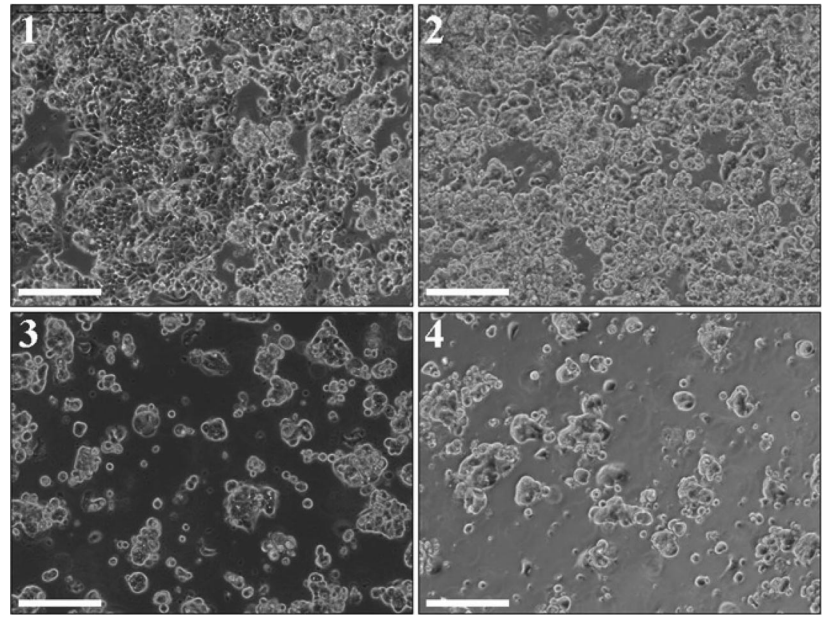

Figure 5. Microscopic visualization of the morphology of live MCF-7 cells incubated with citrate buffer (1), empty buckysomes (2), PEBs (3), and Abraxane (4) for a 72-h time period. The concentration of paclitaxel in images 3 and 4 is 714 ng/ml. These images were collected from the same samples used in the assay shown in Figure 4. The scale bars in all four images are 250 μm.

MATERIALS AND METHODS

Buckysome Preparation: The globular fullerene amphiphile AF-1 was synthesized as previously described.[24] To create buckysomes with a dense, hydrophobic interior, AF-1 (1.5 mg/mL) was hydrated in 10 mM citrate buffer (pH 7.4) for 10 min at 70 °C. During this process, the mixture was subjected to four vortex cycles with a Vortex Genie 2 (G-560, Scientific Industries, Inc., Bohemia, NY) at setting "10" for 30 s. The four vortex cycles were separated by equal time intervals.

To investigate the buckysomes' encapsulation of hydrophobic molecules, the hydrophobic fluorescent probe 1,1′-dioctadecyl-3,3,3′,3′-tetramethylindocarbocyanine perchlorate (DiI, Invitrogen, 10 μg) was added to 1.5 mg/mL AF-1 in 10 mM citrate buffer (pH 7.4) and vortexed under the conditions described above. Excess DiI was separated from the entrapped DiI by means of size exclusion chromatography on a Sephadex G-75 (Sigma-Aldrich, St. Louis, MO) column. The absorbance was measured at 550 nm (Tecan Systems Inc., San Jose, CA) to quantify the amount of DiI encapsulated in the buckysomes. To prepare paclitaxel-embedded buckysomes (PEBs), 0.6 mg/mL paclitaxel was sonicated (Cole-Parmer sonicator (model no. 08849−00), Vernon Hills, IL) for 1 min in 10 mM citrate buffer (pH 7.4). AF-1 was quickly added to this solution at a concentration of 1.5 mg/mL, and PEBs were prepared from the resulting solution using the method described above.

To visualize buckysome internalization in cells, the buckysomes were coupled to 6-aminofluorescein (no. 07985, Fluka-Sigma-Aldrich, St. Louis, MO) using the following procedure. A 400 μL portion of a buckysome solution was incubated with 100 μL each of 0.25 M *N*-ethyl-*N*′- [3- dimethylaminopropyl]carbodiimide (EDC; Fluka) and 0.25 M *N*-hydroxysulfosuccimide (sulfo-NHS; Pierce, Rockford, IL) for 2 h at room temperature. The pH was adjusted to 7.0 using 0.5 M NaOH. To this solution, 300 μL of 6-aminofluorescein (1 mg/mL prepared in dimethyl sulfoxide) was added, and the mixture was incubated overnight at room temperature. The unbound 6-aminofluorescein was separated from 6-aminofluorescein coupled to the buckysomes by size exclusion chromatography on a Sephadex G-75 column. The fractions were analyzed by fluorimetry (Tecan Systems Inc., San Jose, CA) for 6-aminofluorescein emission at 520 nm.

The prepared buckysomes were analyzed by cryogenic electron microscopy (cryo-EM), negative-stained transmission electron microscopy (TEM), and dynamic light scattering (DLS). High performance liquid chromatography (HPLC) was performed on the PEB samples to measure the final concentration of paclitaxel embedded in the buckysomes.

Transmission Electron Microscopy. The buckysomes were visualized using uranyl acetate negative staining. A 400 mesh copper grid coated with carbon film and stabilized with Formvar (no. 01754-F, Ted Pella Inc., Redding, CA) was coated with poly-L-lysine (MW 100−140 kD, Polysciences, Inc., Warrington, PA) prior to sample staining. A 5 μL portion of buckysome sample solution was placed on the grid for 5 min, and excess sample was blotted with filter paper. The samples were then stained with a 1% solution of uranyl acetate for 1 min and allowed to dry. Analysis of the stained grids was performed with a JEOL JEM-1010 transmission electron microscope (Tokyo, Japan) at an accelerating voltage of 80 kV. The images were captured with an AMT Advantage digital CCD camera system.

Cryogenic Electron Microscopy. A 5 μL drop of a buckysome solution was frozen in liquid ethane on a 400 mesh copper grid coated with ultrathin 3 nm carbon (no. 01824, Ted Pella Inc., Redding, CA). Vitrobot (FEI, Holland) was used for automated cryogenic freezing of the grids (1-s hang time, 1 blot, room temperature). The data were collected with a TVIPS (Gauting, Germany) F415 4 K × 4 K slow-scan CCD camera on an FEI (Eindhoven, Holland) Tecnai G^2 TF30 Polara electron microscope operating at 300 kV and at liquid nitrogen temperature by means of a low-dose protocol. The postmagnification value was 1.615 and the CCD pixel size was 15 μm. The micrographs were processed with EMAN v1.7 software (Baylor College of Medicine, Houston, TX).

Dynamic Light Scattering. DLS measurements were performed using a Malvern Nano-ZS zetasizer (Malvern Instruments Ltd., Worcestershire, United Kingdom). The Nano-ZS employs noninvasive back scatter (NIBS) optical technology and measures real-time changes in intensity of scattered light as a result of particles undergoing Brownian motion. The samples were illuminated by a 633 nm He−Ne laser and the scattered light was measured at an angle of 173° using an avalanche photodiode. The size distribution of the buckysomes was calculated from the particle diffusion coefficient according to the Stokes−Einstein equation. The average diameter and the polydispersity index of the buckysomes were calculated by CONTIN analysis software.

High Performance Liquid Chromatography. The paclitaxel was released from the PEBs by diluting the PEBs 1:10 with ethanol. The ethanol−PEB mixture was then analyzed for paclitaxel content using reverse-phase HPLC with UV detection by injecting 50 μL aliquots of the mixture onto a Waters modular HPLC system (Waters Corporation, Milford, MA). The HPLC system consisted of a controller (model no. 600), an autosampler (model no. 717 plus) and a photodiode array detector (model no. 2996). Chromatographic separations were achieved by means of a Waters Symmetry C18 (3.5 μm) column (4.6 mm × 75 mm, part no. WAT 066224). The mobile phase consisted of nanopure water (18 MΩ-cm) and HPLC grade acetonitrile mixed at varying ratios throughout the separation. Specifically, 24% acetonitrile in water was used for 2 min, followed by a linear gradient to 58% acetonitrile over 6 min, then a linear gradient to 70% acetonitrile over 1 min, then a linear gradient to 34% acetonitrile over 1 min and held for 5 min, then a linear gradient to 24% acetonitrile over 2 min and held for 3 min. The mobile phase was delivered at 1 mL/min and UV detection was performed at 227.5 nm. The mobile phase was degassed by bubbling helium gas prior to and during the analysis. Data were acquired and processed using Empower 2 (build 2154) software from Waters Corporation.

***In Vitro* Imaging Using Fluorescence Microscopy.** A431 cells were grown in 8-chamber tissue culture slides and exposed to 6-aminofluorescein-buckysomes for 18 h at 37 °C in a 5% CO_2 environment. After two washes with Dulbecco's phosphate-buffered saline (Gibco), cells were fixed in 4% paraformaldehyde (Sigma-Aldrich) for 20 min and washed twice with Dulbecco's phosphate-buffered saline. The cells were fixed and counterstained with an Image-iT LIVE plasma membrane (AlexaFluor 594) and a nuclear (Hoescht 33342) labeling kit (Invitrogen, Carlsbad, CA). To visualize the hydrophobic probe DiI, macrophages were exposed to DiI-embedded buckysomes for 18 h at 37 °C in a 5% CO_2 environment. After two washes, the cells were fixed with 4% paraformaldehyde and mounted in ProLong Gold antifade reagent with 4′,6-diamidino-2-phenylindole (DAPI; Invitrogen). The chambers were removed and the slides were dried. Images of fixed cells were acquired with an Olympus IX71 inverted microscope (Olympus America Inc., Center Valley, PA) and a Retiga 2000R Camera (Q Imaging, Burnaby, BC, Canada). Images were processed using Compix SimplePCI software (Compix Inc., Sewickley, PA).

Cell Culture for Cytotoxicity Studies. MCF7 breast cancer cells (HTB-22), mouse macrophage-like monocytes (TIB-67) and A431 human epidermoid carcinoma cells (CRL-1555) were obtained from American type Culture Collection (ATCC, Manassas, VA). MCF7 cells were grown in Eagle's minimum essential medium (EMEM; ATCC) supplemented with 10% fetal bovine serum (Gibco), 0.01 mg/mL bovine insulin (Sigma-Aldrich, St. Louis, MO), and 1% antibiotics which included 2 mM L-glutamine, 100 μg/mL penicillin, and 100 U/mL streptomycin (Sigma-Aldrich). Macrophages and A431 cells were grown in Dulbecco's Modified Eagle's Medium (DMEM; ATCC) supplemented with 10% fetal bovine serum and 1% antibiotics. All cells were grown at 37 °C in a 5% CO_2 environment.

Cytotoxicity Studies. MCF-7 cells were seeded in triplicate into tissue-treated 12-well plates (Bector Dickinson, Franklin Lakes, NJ) totaling 1.0×10^5 cells/well and allowed to attach overnight. Abraxane (Abraxis Bioscience Inc., Los Angeles, CA) was provided as a gift from The University of Texas M.D. Anderson Cancer Center, Houston. Abraxane and PEBs containing 0.0286, 0.1429, and 0.7143 μg/mL paclitaxel were added to the cells. For control studies, empty buckysomes and plain citrate buffer (pH 7.4, 0.476 mM) were also added to cells. The final concentration of AF-1 was 59.52 μg/mL in both the controls (PEBs and the empty buckysomes). The cells were incubated in two sepa-

rate groups for 48 and 72 h. After the desired time intervals, cells were harvested using 0.25% trypsin-EDTA (Gibco). The cell viability was then determined with a Beckman Coulter Vi-Cell XR system (Beckman Coulter, Fullerton, CA).

Acknowledgment. This work was supported by grants from NASA (NNJ05HE75A), DoD/TATRC (W81XWH-04-20035T5), and DoD/TATRC (DAMD17-01-2-0047). We acknowledge Dr. Michael Kellermann in the laboratory of Dr. Andreas Hirsch for synthesis of AF-1. We thank Dr Angel Paredes at the Structural Biology Research Center, University of Texas Health Science Center, Houston, TX for assistance with the cryo-electron microscope and Mr. Kenneth Dunner, Jr. at The University of Texas M.D. Anderson Cancer Center, Houston, TX (Cancer Center Core Grant CA16671) for help with the transmission electron microscope. We thank Dr. Brigitte Papahadjopoulos-Sternberg at Nano Analytical Laboratory, San Francisco, CA for assistance with freeze-fracture microscopy, and we thank Drs. Russ Lebovitz, Gabriel Lopez, and Anil Sood for discussions concerning the manuscript.

Supporting Information Available: DLS and HPLC data for buckysomes. This material is available free of charge *via* the Internet at http://pubs.acs.org.

REFERENCES AND NOTES

1. Ferrari, M. Cancer Nanotechnology: Opportunities and Challenges. *Nat. Rev. Cancer* **2005**, *5*, 161–171.
2. Storm, G.; Crommelin, D. J. A. Liposomes: *Quo Vadis*. *Pharm. Sci. Technol. Today* **1998**, *1*, 19–31.
3. Kao, C.-Y.; Hoffman, E. A.; Beck, K. C.; Bellamkonda, R. V.; Annapragada, A. V. Long-Residence-Time Nano-Scale Liposomal Iohexol for X-Ray-Based Blood Pool Imaging. *Acad. Radiol.* **2003**, *10*, 475–483.
4. Mukundan, S., Jr.; Ghaghada, K. B.; Badea, C. T.; Kao, C.-Y.; Hedlund, L. W.; Provenzale, J. M.; Johnson, G. A.; Chen, E.; Bellamkonda, R. V.; Annapragada, A. A Liposomal Nanoscale Contrast Agent for Preclinical CT in Mice. *Am. J. Roentgenol.* **2006**, *186*, 300–307.
5. Lasic, D. D.; Papahadjopoulos, D. Liposomes Revisited. *Science* **1995**, *267*, 1275–1276.
6. Thanyani, S. T.; Roberts, V.; Siko, D. G. R.; Vrey, P.; Verschoor, J. A. A Novel Application of Affinity Biosensor Technology to Detect Antibodies to Mycolic Acid in Tuberculosis Patients. *J. Immunol. Methods* **2008**, *332*, 61–72.
7. Torchilin, V. P. Multifunctional Nanocarriers. *Adv. Drug Delivery Rev.* **2006**, *58*, 1532–1555.
8. Dhanikula, A. B.; Panchagnula, R. Preparation and Characterization of Water-Soluble Prodrug, Liposomes and Micelles of Paclitaxel. *Curr. Drug Delivery* **2005**, *2*, 75–91.
9. Yang, T.; Choi, M.-K.; Cui, F.-D.; Kim, J. S.; Chung, S.-J.; Shim, C.-K.; Kim, D.-D. Preparation and Evaluation of Paclitaxel-Loaded PEGylated Immunoliposome. *J. Controlled Release* **2007**, *120*, 169–177.
10. Yang, T.; Cui, F.-D.; Choi, M.-K.; Cho, J.-W.; Chung, S.-J.; Shim, C.-K.; Kim, D.-D. Enhanced Solubility and Stability of PEGylated Liposomal Paclitaxel: *In vitro* and *in vivo* Evaluation. *Int. J. Pharm.* **2007**, *338*, 317–326.
11. Yang, T.; Choi, M.-K.; Cui, F.-D.; Lee, S.-J.; Chung, S.-J.; Shim, C.-K.; Kim, D.-D. Antitumor Effect of Paclitaxel-Loaded PEGylated Immunoliposomes Against Human Breast Cancer Cells. *Pharm. Res.* **2007**, *24*, 2402–2411.
12. Yang, T.; Cui, F.-D.; Choi, M.-K.; Lin, H.; Chung, S.-J.; Shim, C.-K.; Kim, D.-D. Liposome Formulation of Paclitaxel with Enhanced Solubility and Stability. *Drug Delivery* **2007**, *14*, 301–308.
13. Peltier, S.; Oger, J.-M.; Lagarce, F.; Couet, W.; Benoit, J.-P. Enhanced Oral Paclitaxel Bioavailability After Administration of Paclitaxel-Loaded Lipid Nanocapsules. *Pharm. Res.* **2006**, *23*, 1243–1250.
14. Oberdorster, E. Manufactured Nanomaterials (Fullerenes, C_{60}) Induce Oxidative Stress in the Brain of Juvenile Largemouth Bass. *Environ. Health Perspect.* **2004**, *112*, 1058–1062.
15. Zhu, S.; Oberdorster, E.; Haasch, M. L. Toxicity of an Engineered Nanoparticle (Fullerene, C60) in Two Aquatic Species, Daphnia and Fathead Minnow. *Mar. Environ. Res.* **2006**, *62* (Suppl.), S5–9.
16. Gharbi, N.; Pressac, M.; Hadchouel, M.; Szwarc, H.; Wilson, S. R.; Moussa, F. [60]Fullerene is a Powerful Antioxidant *in vivo* with No Acute or Subacute Toxicity. *Nano Lett.* **2005**, *5*, 2578–2585.
17. Zhou, S.; Burger, C.; Chu, B.; Sawamura, M.; Nagahama, N.; Toganoh, M.; Hackler, U. E.; Isobe, H.; Nakamura, E. Spherical Bilayer Vesicles of Fullerene-Based Surfactants in Water: A Laser Light Scattering Study. *Science* **2001**, *291*, 1944–1947.
18. Georgakilas, V.; Pellarini, F.; Prato, M.; Guldi, D. M.; Melle-Franco, M.; Zerbetto, F. Supramolecular Self-Assembled Fullerene Nanostructures. *Proc. Natl. Acad. Sci. U.S.A.* **2002**, *99*, 5075–5080.
19. Liu, Y.; Xiao, S.; Li, H.; Li, Y.; Liu, H.; Lu, F.; Zhuang, J.; Zhu, D. Self-Assembly and Characterization of A Novel Hydrogen-Bonded Nanostructure. *J. Phys. Chem. B* **2004**, *108*, 6256–6260.
20. Guldi, D. M.; Zerbetto, F.; Georgakilas, V.; Prato, M. Ordering Fullerene Materials at Nanometer Dimensions. *Acc. Chem. Res.* **2005**, *38*, 38–43.
21. Brettreich, M.; Hirsch, A. A Highly Water-Soluble Dendro[60]fullerene. *Tetrahedron Lett.* **1998**, *39*, 2731–2734.
22. Maierhofer, A. P.; Brettreich, M.; Burghardt, S.; Vostrowsky, O.; Hirsch, A.; Langridge, S.; Bayerl, T. M. Structure and Electrostatic Interaction Properties of Monolayers of Amphiphilic Molecules Derived from C_{60}-Fullerenes: A Film Balance, Neutron-, and Infrared Reflection Study. *Langmuir* **2000**, *16*, 8884–8891.
23. Brettreich, M.; Burghardt, S.; Bottcher, C.; Bayerl, T.; Bayerl, S.; Hirsch, A. Globular Amphiphiles: Membrane-Forming Hexaadducts of C_{60}. *Angew. Chem., Int. Ed.* **2000**, *39*, 1845–1848.
24. Braun, M.; Atalick, S.; Guldi, D. M.; Lanig, H.; Brettreich, M.; Burghardt, S.; Hatzimarinaki, M.; Ravanelli, E.; Prato, M.; van Eldik, R.; *et al.* Electrostatic Complexation and Photoinduced Electron Transfer between Zn-Cytochrome *c* and Polyanionic Fullerene Dendrimers. *Chem.—Eur. J.* **2003**, *9*, 3867–3875.
25. Burghardt, S.; Hirsch, A.; Schade, B.; Ludwig, K.; Boettcher, C. Switchable Supramolecular Organization of Structurally Defined Micelles based on an Amphiphilic Fullerene. *Angew. Chem., Int. Ed.* **2005**, *44*, 2976–2979.
26. Partha, R.; Lackey, M.; Hirsch, A.; Casscells, S. W.; Conyers, J. L. Assembly of Amphiphilic C_{60} Fullerene Derivatives into Nanoscale Supramolecular Structures. *J. Nanobiotechnol.* **2007**, *5*, 1–11.
27. Rowinsky, E. K.; Donehower, R. C. Paclitaxel (Taxol). *New Engl. J. Med.* **1995**, *332*, 1004–1014.
28. Mekhail, T. M.; Markman, M. Paclitaxel in Cancer Therapy. *Expert Opin. Pharmacother.* **2002**, *3*, 755–766.
29. Crosasso, P.; Ceruti, M.; Brusa, P.; Arpicco, S.; Dosio, F.; Cattel, L. Preparation, Characterization and Properties of Sterically Stabilized Paclitaxel-Containing Liposomes. *J. Controlled Release* **2000**, *63*, 19–30.
30. Sharma, A.; Sharma, U. S.; Straubinger, R. M. Paclitaxel-Liposomes for Intracavitary Therapy of Intraperitoneal P388 Leukemia. *Cancer Lett.* **1996**, *107*, 265–272.
31. Singla, A. K.; Garg, A.; Aggarwal, D. Paclitaxel and its Formulations. *Int. J. Pharm.* **2002**, *235*, 179–192.
32. Gelderblom, H.; Verweij, J.; Nooter, K.; Sparreboom, A. Cremophor EL: The Drawbacks and Advantages of Vehicle Selection for Drug Formulation. *Eur. J. Cancer* **2001**, *37*, 1590–1598.
33. Schnyder, A.; Huwyler, J. Drug Transport to Brain with Targeted Liposomes. *NeuroRx* **2005**, *2*, 99–107.
34. Dubochet, J.; Adrian, M.; Chang, J. J.; Homo, J. C.; Lepault, J.; McDowall, A. W.; Schultz, P. Cryo-Electron Microscopy of Vitrified Specimens. *Q. Rev. Biophys.* **1988**, *21*, 129–228.

35. Lasic, D. D.; Frederik, P. M.; Stuart, M. C. A.; Barenholz, Y.; McIntosh, T. J. Gelation of Liposome Interior. A Novel Method for Drug Encapsulation. *FEBS Lett.* **1992**, *312*, 255–258.
36. Frederik, P. M.; Hubert, D. H. W. Cryoelectron Microscopy of Liposomes. *Methods Enzymol.* **2005**, *391*, 431–448.
37. Sulkowski, W. W.; Pentak, D.; Nowak, K.; Sulkowska, A. The Influence of Temperature and pH on the Structure of Liposomes Formed from DMPC. *J. Mol. Struct.* **2006**, *792−793*, 257–264.
38. Ellens, H.; Bentz, J.; Szoka, F. C. Destabilization of Phosphatidylethanolamine Liposomes at the Hexagonal Phase Transition Temperature. *Biochemistry* **1986**, *25*, 285–294.
39. Israelachvili, J. N.; Mitchell, D. J.; Ninham, B. W. Theory of Self-Assembly of Lipid Bilayers and Vesicles. *Biochim. Biophys. Acta* **1977**, *470*, 185–201.
40. Gulik-Krzywicki, T.; Dedieu, J. C.; Roux, D.; Degert, C.; Laversanne, R. Freeze-Fracture Electron Microscopy of Sheared Lamellar Phase. *Langmuir* **1996**, *12*, 4668–4671.
41. Hoppe, W.; Hegerl, R. Three-Dimensional Structure Determination by Electron Microscopy (Non-Periodic Specimens). In *Computer Processing of Electron Microscope Images*, Hawkes, P. W., Ed.; Springer-Verlag: Berlin, 1980; pp 127−185..
42. Jiang, Q.-X.; Chester, D. W.; Sigworth, F. J. Spherical Reconstruction: A Method for Structure Determination of Membrane Proteins from Cryo-EM Images. *J. Struct. Biol.* **2001**, *133*, 119–131.
43. Lucic, V.; Leis, A.; Baumeister, W. Cryo-Electron Tomography of Cells: Connecting Structure and Function. *Histochem Cell Biol.* **2008**, *130*, 185–196.
44. Hirai, M.; Iwase, H.; Hayakawa, T.; Koizumi, M.; Takahashi, H. Determination of Asymmetric Structure of Ganglioside-DPPC Mixed Vesicle using SANS, SAXS, and DLS. *Biophys. J.* **2003**, *85*, 1600–1610.
45. Park, S.-H.; Oh, S.-G.; Mun, J.-Y.; Han, S.-S. Loading of Gold Nanoparticles Inside the DPPC Bilayers of Liposome and Their Effects on Membrane Fluidities. *Colloids Surf. B* **2006**, *48*, 112–118.
46. Jordan, M. A.; Wilson, L. Microtubules as a Target for Anticancer Drugs. *Nat. Rev. Cancer* **2004**, *4*, 253–265.
47. Desai, N. P.; Louie, L.; Ron, N.; Magdassi, S.; Soon-Shiong, P. *Protein-Based Nanoparticles for Drug Delivery of Paclitaxel.* Transactions of the Sixth World Biomaterials Congress; Society for Biomaterials: Mt. Laurel, NJ, 2000; *Vol. 1*, p 199.
48. Ibrahim, N. K.; Desai, N.; Legha, S.; Soon-Shiong, P.; Theriault, R. L.; Rivera, E.; Esmaeli, B.; Ring, S. E.; Bedikian, A.; Hortobagyi, G. N.; *et al.* Phase I and Pharmacokinetic Study of ABI-007, a Cremophor-Free, Protein-Stabilized, Nanoparticle Formulation of Paclitaxel. *Clin. Cancer Res.* **2002**, *8*, 1038–1044.
49. Huang, L.; Connor, J.; Wang, C. Y. pH-Sensitive Immunoliposomes. *Methods Enzymol.* **1987**, *149*, 88–99.
50. Mastrobattista, E.; Koning, G. A.; Storm, G. Immunoliposomes for the Targeted Delivery of Antitumor Drugs. *Adv. Drug Delivery Rev.* **1999**, *40*, 103–127.
51. Kirpotin, D.; Park, J. W.; Hong, K.; Zalipsky, S.; Li, W.-L.; Carter, P.; Benz, C. C.; Papahadjopoulos, D. Sterically Stabilized Anti-HER2 Immunoliposomes: Design and Targeting to Human Breast Cancer Cells *in vitro*. *Biochemistry* **1997**, *36*, 66–75.
52. Miller, C. R.; Bondurant, B.; McLean, S. D.; McGovern, K. A.; O'Brien, D. F. Liposome-Cell Interactions in Vitro: Effect of Liposome Surface Charge on the Binding and Endocytosis of Conventional and Sterically Stabilized Liposomes. *Biochemistry* **1998**, *37*, 12875–12883.
53. Siwak, D. R.; Tari, A. M.; Lopez-Berestein, G. The Potential of Drug-Carrying Immunoliposomes as Anticancer Agents. *Clin. Cancer Res.* **2002**, *8*, 955–956.
54. Greish, K. Enhanced Permeability and Retention of Macromolecular Drugs in Solid Tumors: A Royal Gate for Targeted Anticancer Nanomedicines. *J. Drug Target.* **2007**, *15*, 457–464.
55. Adis Data Information, B. V. ABI 007. Adis R&D Profile. *Drugs R&D* **2004**, *5*, 155–159.
56. Scripture, C. D.; Figg, W. D.; Sparreboom, A. Paclitaxel Chemotherapy: From Empiricism to a Mechanism-Based Formulation Strategy. *Ther. Clin. Risk Manage.* **2005**, *1*, 107–114.
57. Gradishar, W. J. Albumin-Bound Paclitaxel: A Next-Generation Taxane. *Expert Opin. Pharmacother.* **2006**, *7*, 1041–1053.
58. Hawkins, M. J.; Soon-Shiong, P.; Desai, N. Protein Nanoparticles as Drug Carriers in Clinical Medicine. *Adv. Drug Delivery Rev.* **2008**, *60*, 876–885.
59. Russo, J.; Soule, H. D.; McGrath, C.; Rich, M. A. Reexpression of the Original Tumor Pattern by a Human Breast Carcinoma Cell Line (MCF-7) in Sponge Culture. *J. Natl. Cancer. Inst.* **1976**, *56*, 279–282.